Nuclear modification factors at forward rapidities

D. Röhrich[a]

[a]University of Bergen, Norway

The nuclear modification factor for d+Au collisions at $\sqrt{s_{NN}} = 200$ GeV changes from a Cronin-like enhancement of pions (and charged hadrons) at midrapidity to an increasing suppression at forward rapidities. In central Au+Au collisions at 200 GeV a strong pion suppression is observed in R_{AuAu} at all rapidities, while protons are enhanced at all rapidities. The nuclear modification factor does not depend on rapidity.

1. NUCLEAR MODIFICATION FACTOR

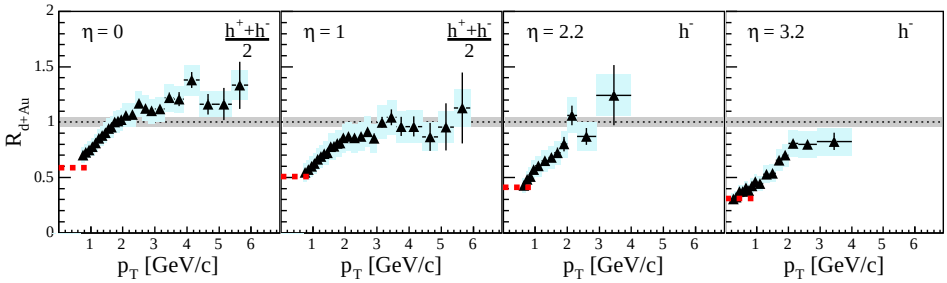

Figure 1. Nuclear modification factor for charged hadrons at pseudorapidities = 0, 1.0, 2.2, 3.2. One standard deviation statistical errors are indicated by error bars. Systematic errors are shown with shaded boxes. The shaded band around unity indicates the estimated error on the normalization to the number of collisons.

The high-p_{T} spectra of particles produced in nuclear collisions are subject to various initial and final state effects. Initial state effects like the Cronin effect enhance the yield in p+A and A+A collisions as compared to nucleon-nucleon reactions at intermediate transverse momenta, nuclear shadowing and gluon saturation suppress the yield. Parton energy loss due to gluon bremsstrahlung during their passage through a dense medium with free color charges - created in central Au+Au collisions - suppresses the hadron yield at high-p_{T}. This final state effect is also called jet-quenching. The degree of suppression/enhancement is quantified by means of the nuclear modification factor R_{AA} using p+p reference spectra scaled up with the average number N_{coll} of binary nucleonic collisions in the heavy-ion system:

$$R_{AA} = \left(d^2N_{AA}/dydp_{\mathrm{T}}\right) / \left(N_{coll} \cdot d^2N_{pp}/dydp_{\mathrm{T}}\right) \quad (1)$$

Another measure is

$$R_{CP} = \left(N_{coll}^{peripheral} \cdot d^2N_{AA}^{central}/dydp_{\rm T}\right) / \left(N_{coll}^{central} \cdot d^2N_{AA}^{peripheral}/dydp_{\rm T}\right). \quad (2)$$

Both observables quantify the modifaction of the transverse momentum spectra in central collisions, however, they are not identical: R_{AA} suffers from iso-spin effects and the canonical strangeness suppression of the reference; in the case of R_{CP} residual collective effects are present in the reference.

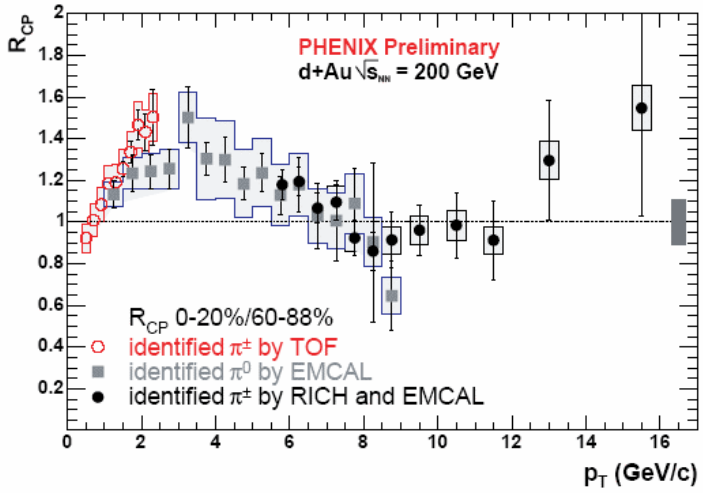

Figure 2. R_{CP} for pions in d+Au at 200 GeV [6]. The shaded band on the right represents the overall fractional systematic uncertainty due to N_{coll}.

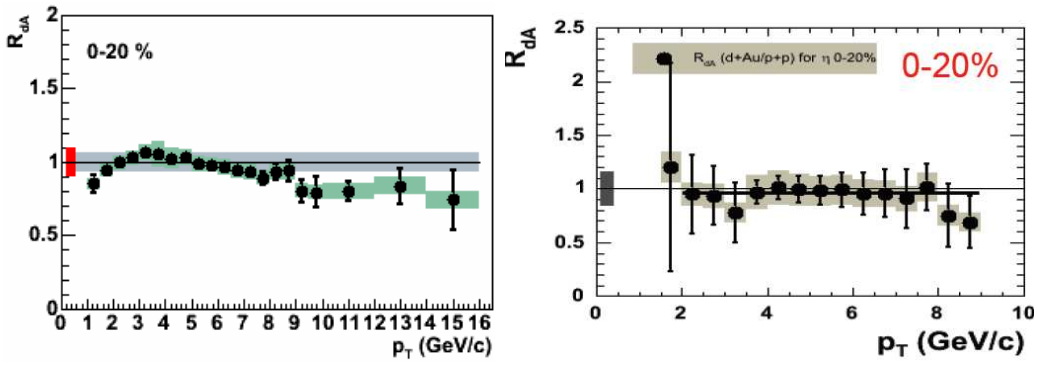

Figure 3. Left panel: R_{dAu} for π^0 at midrapidity for central d+Au collisions. Right panel: R_{dAu} for η at midrapidity for central d+Au collisions. (PHENIX data [7]).

Next-to-Leading Order (NLO) leading-twist perturbative-QCD (pQCD) calculations of inclusive hadron production describe pion production in p+p collisions at RHIC at

$\sqrt{s_{NN}} = 200$ GeV reasonably well. They agree with π^0 data at central rapidity and with data at forward rapidities, although there are sizable uncertainties in the NLO calculation related to the choice of fragmentation functions.

Hadrons produced in nuclear collisions like d+Au at forward rapidities and at high-$p_{\rm T}$ probe partons in the Au-nucleus that carry only a small fraction of the momentum (x_2) of the initial hadron. The kinematics of $2 \rightarrow 1$ processes shows that x_2 can be as small as $3.5 \cdot 10^{-4}$, however, the more general $2 \rightarrow 2$ interaction kinematics folded with parton distribution functions shows that mainly partons with $x_2 = 0.01$ contribute to the cross section for pions with $p_{\rm T} = 1.5$ GeV/c and $\eta = 3.2$ [1].

2. NUCLEAR MODIFICATION FACTORS FOR COLD NUCLEAR MATTER

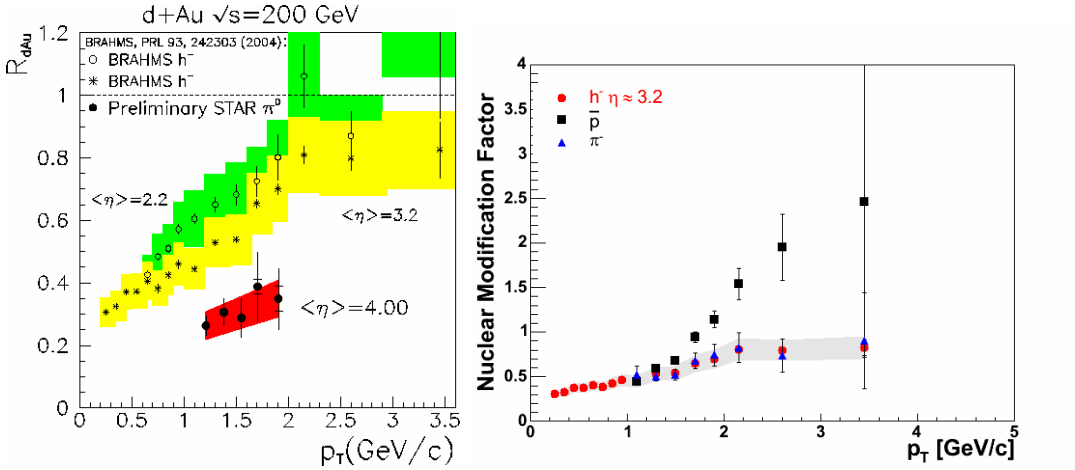

Figure 4. R_{dAu} at forward rapidities. Left panel: π^0 at $\eta = 4$ (STAR [8]). Right panel: π^- and antiprotons at $\eta = 3.2$ (BRAHMS [9]).

The nuclear modification factor R_{dAu} for charged hadrons have been measured over a wide range of rapidities: from midrapidity to $\eta = 3.2$. At midrapidity, both R_{dAu} and R_{CP} have been determined for many identified hadrons, while at forward rapidity only data for π^-, π^0 and antiprotons exist (J/Ψ will not be discussed here).

2.1. Charged hadrons in d+Au collisions

Particle production at forward rapidities probes partons at smaller x scales. Suppression effects due to nuclear shadowing and/or gluon saturation are expected in d+Au collisions at large y. Fig. 1 shows the nuclear modification factor R_{dAu} for minimum bias d+Au events as a function of p_T and η [2] (see also [3–5]). R_{dAu} rises with p_T and falls with η. At midrapidity, R_{dAu} goes above 1. The so-called Cronin enhancement at $\eta = 0$ has been attributed to multiple scattering of the incoming partons during the collision. At more forward rapidities the data show a suppression of the hadron yields.

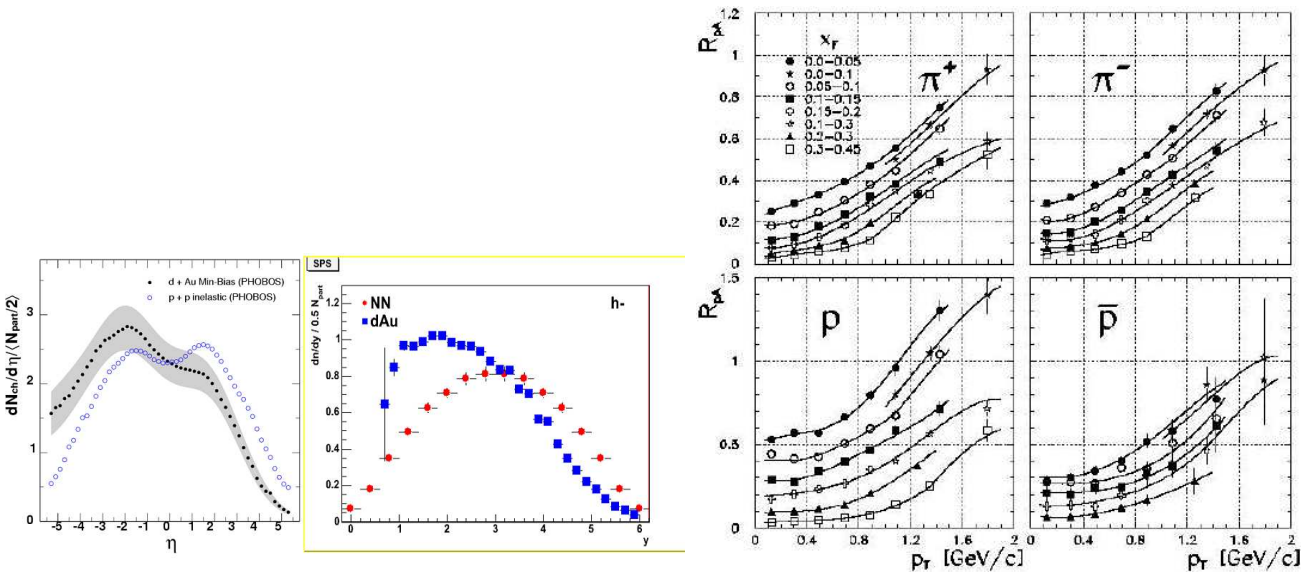

Figure 5. Left panel: Pseudorapidity distributions of charged particles in d+Au and p+p (nucleon-nucleon NN), scaled by the number of participant-pairs, both at RHIC (left) and at SPS (right) energies [12,13]. Right panel: R_{pPb} for pions and (anti-)protons at forward rapidities measured at different x_F for p+Pb collisions at the SPS [14].

2.2. Identified hadrons in d+Au collisions

The difference of R_{CP} and R_{dAu} and their dependence on the particle species can be best studied at midrapidity. Fig. 2 shows R_{CP}, the ratio of point-like scaled central to peripheral collisions for pions in d+Au at 200 GeV [6]. The shaded band on the right represents the overall fractional systematic uncertainty due to N_{coll}. The data show binary scaling at high p_T and a clear Cronin effect at intermediate p_T.

Fig. 3 shows the nuclear modification factor R_{dAu} for π^0 (left) and for η (right) at midrapidity for central d+Au collisions [7]. Surprisingly, almost no Cronin effect is observed and R_{dAu} is consistent with unity - except for very large p_T where R_{dAu} for pions is slightly lower than 1. PHENIX [10] and STAR [11] have reported a strong Cronin effect for mesons (charged hadrons: pions, kaons, Φ) and baryons (protons and Λ), visible in both R_{dAu} and R_{CP}; the strength of the effect seems to be larger for baryons.

Fig. 4 shows the nuclear modification factor R_{dAu} at forward rapidities: π^0 at $\eta = 4$ (STAR [8]) and data on π^- and antiprotons at $\eta = 3.2$ (BRAHMS [9]). Pions are clearly suppressed and the effect increases with rapidity. Antiprotons show an enhancement. It has to be noted that this enhancement is not seen in R_{CP}.

2.3. Comparison with p+A data at SPS

The suppression at forward rapidities is already visible in the pseudorapidity distributions of charged particles in d+Au and p+p (nucleon-nucleon), scaled by the number of participant-pairs, both at RHIC and at SPS energies [12,13]. Fig. 5 shows a similar trend at both energies: an enhanced production at $\eta \leq 0$ and a suppression at $\eta \geq 0$; the

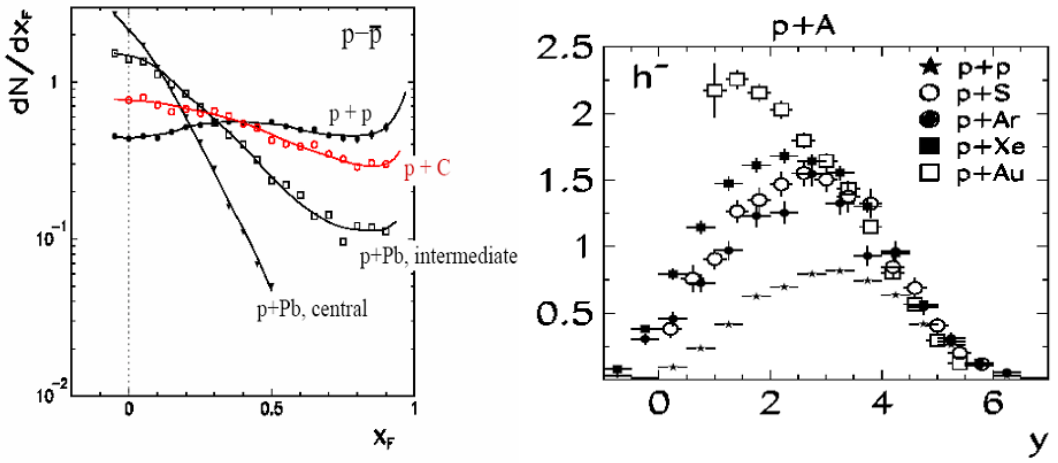

Figure 6. Left panel: Stopping at SPS [15]: net protons yield as a function of x_F for varions nuclear collisions [15]. Right panel: Rapidity distribution of negatively charged hadrons in nuclear collisions at SPS [13].

nuclear modification effects all pions, not only at high p_T. R_{pPb} at SPS exhibits a similar suppression trend, the suppression increases with increasing x_F [14]. At SPS, there is a simple explanation for this effect: due to the large momentum degradation of the projectile in (central) pA collisions by multiple collisions (see Fig. 6, left panel) - which is very different from p+p - successive collisions pile-up pions close to midrapidity, but at forward rapidities the pion yield is independent of the target (see Fig. 6, right panel) [16]. It seems that the first collision is equally effective in producing pions in all reactions, resulting in a suppression when scaling to pp.

2.4. Initial and final state effects in cold nuclear matter

2.4.1. CGC saturation models

Saturation effects should increase with the thickness of nuclear material traversed by the incoming probe and indeed we see a greater suppression for more central collisions [2]. Both, R_{dAu} and R_{CP}, as well as the pseudorapidity distribution of charged hadrons and the invariant cross section of π^0 production in d+Au collisions at RHIC can be quantitatively described by gluon saturation within the framework of a Color Glass Condensate (Fig. 7) [17,18].

2.4.2. pQCD models

At higher p_T pQCD based models which implement a Glauber-type collision geometry and include the standard nuclear shadowing and initial state incoherent multiple scattering agree reasonably well with the measured R_{dAu} (Fig. 8, left) and cannot be ruled out [19] (see also [20]). However, the centrality dependence of R_{CP} is underestimated [21] and there are doubts that nuclear shadowing is strong enough to describe the data [1,22]. On the other hand, coherent multiple scattering of a parton with the remnants of the nucleus in the final state can create an additional suppression at low and intermediate p_T which grows with rapidity and centrality (Fig. 8, right) [23].

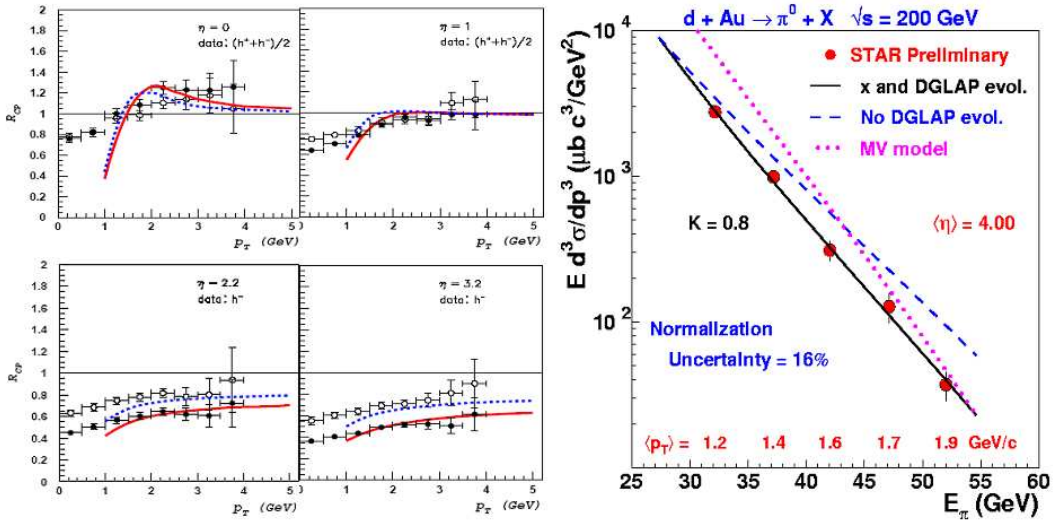

Figure 7. Left panel: Comparison of a CGC calculation [17] for R_{CP} with BRAHMS data. Right panel: Comparison of a CGC calculation [18] for the π^0 invariant cross section with STAR data.

2.4.3. Phenomenological models

R_{dAu} has been studied in the framework of Gribov-Regge field theory [24], where shadowing in d+Au collisions is linked to diffraction. A parametrized gluonic parton distribution function (data from H1 and ZEUS) can describe the suppression at forward rapidities at RHIC. Applying this model to SPS data, gluonic shadowing, although present at SPS, cannot explain the observed suppression effect at large x_F. At SPS energies, shadowing due to valence quarks will dominate in this kinematical region. In general, the large x_F region is dominated by the fragmentation of valence quarks, which may suffer from an induced energy loss via increased gluon bremsstrahlung in cold nuclear matter [25]. In addition, momentum conservation at $x_F \rightarrow 1$ and final state multiple scattering might modify R_{dAu} and R_{CP} (Fig. 9) [25,26].

3. FINAL STATE EFFECTS IN CENTRAL NUCLEUS-NUCLEUS COLLISIONS

Pion (and charged hadron) transverse momentum spectra at midrapidity in central Au+Au collisions at 200 GeV show a strong suppression at intermediate and high p_T as compared to properly scaled p+p interactions. This effect is attributed to the energy loss partons suffer while traversing the hot and dense medium produced in these collisions (see [28] and references therein; see also [29]). Data for the lighter Cu+Cu system and at 63 GeV have been presented at this conference. Here we will focus on the rapidity dependence of R_{AuAu} for identified pions and protons in central Au+Au collisions at 200 GeV.

Fig. 10 summarizes the results at midrapidity. The nuclear modification factor for direct photons shows no suppression and is consistent with 1 at all p_T; mesons are suppressed at intermediate and high p_T [7]. Baryons - especially strange baryons - show an enhancement

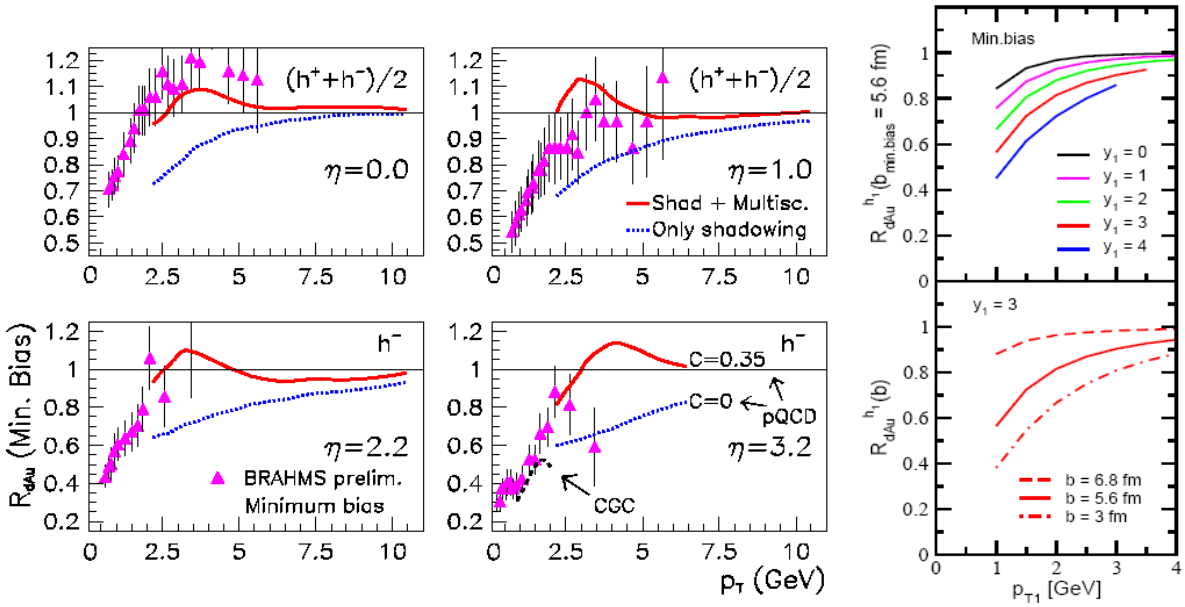

Figure 8. Left panel: pQCD-improved parton model [19] compared to BRAHMS data. Right panel: Rapidity and centrality dependence of suppression effects due to coherent multiple scattering of a parton with the remnants of the nucleus in the final state [23].

in R_{AuAu}, while in R_{CP} both mesons and baryons are suppressed [30].

Fig. 11 compares the (preliminary) nuclear modification factor for pions (left) and protons (right) at midrapidity to the one at forward rapidities [31–34] (central Au+Au collisions). The pions are clearly suppressed, protons are enhanced and there is no dependence on rapidity.

The lack of the rapidity dependence is somewhat surprising since the bulk properties of matter change considerably when going to forward rapidity: the rapidity density of pions drops by a factor of three [35], the radial flow velocity decreases by 30% [36] and the hadron chemistry becomes "SPS-like" [37,38]. However, a 3D-hydrodynamical simulation starting from a CGC initial condition and including jets [39] can describe both the bulk properties as well as R_{AuAu}. The drop of the CGC initial parton distribution by a factor of two (Fig. 12, left) and the different time evolution of the thermalized parton density (Fig. 12, middle) - resulting in less jet energy loss at $\eta = 3.2$ -, is compensated by a steeper p_T-slope of the pQCD components at forward rapidities (Fig. 12, right). An alternative explanation for the constant R_{AuAu} could be that the medium at RHIC is so dense that only particles produced close to the surface can escape and that therefore the corona effect masks the lower parton density at $\eta = 3.2$ [40].

4. CONCLUSION

Although the Cronin effect has been observed both in R_{dAu} and R_{CP} at midrapidity for d+Au collisions at 200 GeV, its magnitude and dependence on the species and on the choice of the reference spectrum needs experimental clarification. Suppression phenomena at forward rapidities have been seen at RHIC and SPS; a variety of processes can

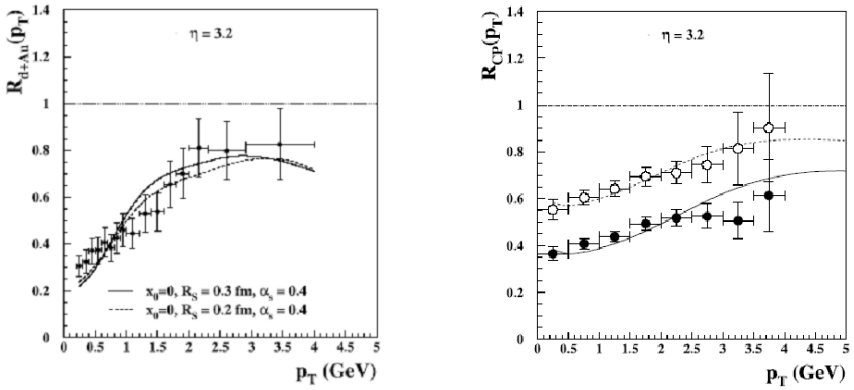

Figure 9. Suppression due to large x_F effects [25]: R_{dAu} and R_{CP} together with BRAHMS data.

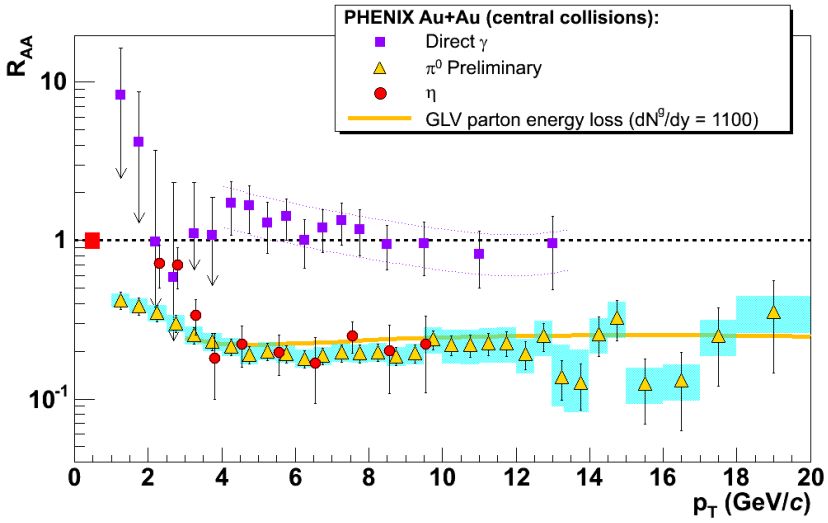

Figure 10. R_{AuAu} for direct photons, π^0 and η produced in central Au+Au collisions at 200 GeV (PHENIX data) [7].

result in suppression. The quality of data is insufficient for ruling out models; back-to-back azimuthal correlations with a large rapidity gap might be able to shed light on the underlying processes [8]. A low energy d+Au run at RHIC would offer a unique chance to study suppression effects at large x_F in detail.

A strong pion suppression is observed at all rapidities in central Au+Au collisions at 200 GeV, while protons are enhanced at all rapidities (R_{AuAu}). The nuclear modification factor does not depend on rapidity.

REFERENCES

1. V. Guzey, M. Strikman and W. Vogelsang, Phys. Lett. **B603** (2004) 173-183.
2. I. Arsene *et al.* (BRAHMS collaboration), Phys. Rev. Lett. **93** (2004) 242303.
3. B.B. Back *et al.* (PHOBOS collaboration), Phys. Rev. **C70** (2005) 061901(R).

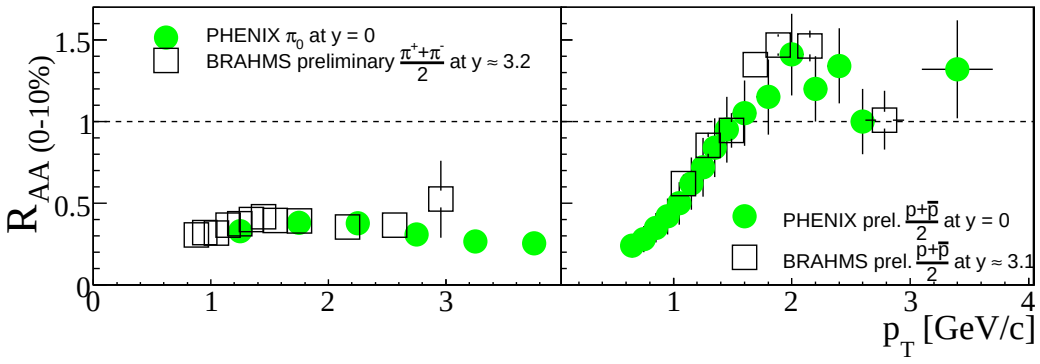

Figure 11. Preliminary R_{AuAu} for pions (left) and protons (right) at y=0 and y=3 (central Au+Au collisions).

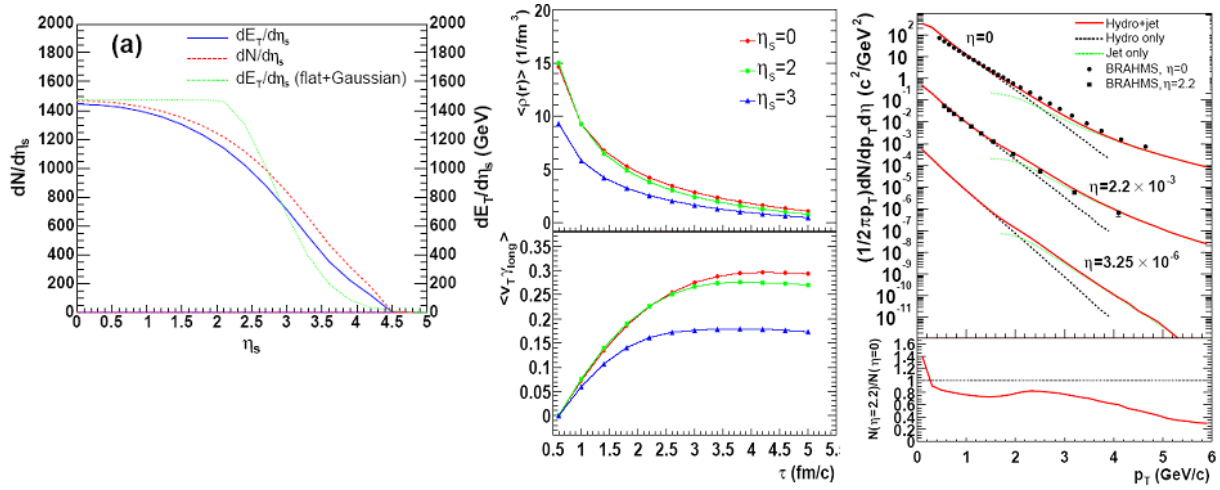

Figure 12. Rapidity dependence of the CGC initial parton distribution (left), time evolution of the thermalized parton density (middle) and p_T-slope of the pQCD components (right) in a 3D-hydrodynamical model [39].

4. S.S. Adler *et al.* (PHENIX collaboration), Phys. Rev. Lett. **94** (2005) 082302.
5. B. Mohanty (STAR collaboration), these Proceedings.
6. K. Adcox *et al.* (PHENIX collaboration), Nucl. Phys. **A757** (2005) 184.
7. B. Cole (PHENIX collaboration), these Proceedings.
8. G. Rakness *et al.* (STAR collaboration), hep-ex/0507093.
9. F. Videbaek *et al.* (BRAHMS collaboration), nucl-ex/0508013.
10. D. Pal *et al.* (PHENIX collaboration), these Proceedings.
11. C. Mironov *et al.* (STAR collaboration), 2005 RHIC&AGS Annual User's Meeting.
12. R. Noucier *et al.* (PHOBOS collaboration), J. Phys. **G30** (2004) S1133.
13. T. Alber *et al.* (NA35 collaboration), Eur. Phys. J. **C2** (1998) 643.
14. B. Boimska (NA49 collaboration), PhD thesis, Warzaw (2004).
15. A. Rybicki (NA49 collaboration), J. Phys. **G30** (2004) S743-S750.

16. S. Brodsky *et al.*, Phys. Rev. Lett. **93** (1977) 1120.
17. D. Kharzeev, Y. V. Kovchegov and K. Tuchin, Phys. Lett. **B599** (2004) 23-31; D. Kharzeev, E. Levin and M. Nardi, Nucl. Phys. **A730** (2004) 448-459, erratum-ibid. **A743** (2004) 329-331.
18. A. Dumitru, A. Hayashigaki and J. Jalilian-Marian, hep-ph/0506308.
19. G. G. Barnafoldi, G. Papp and P. Levai, J. Phys. **G30** (2004) S1125-S1128.
20. A. Arccadi and M. Gyulassy, J. Phys. **G30** (2004) S969-S974.
21. R. Vogt, Phys. Rev. **C70** (2004) 064902.
22. L. Frankfurt, V. Guzey and M. Strikman, Phys. Rev. **D71** (2005) 054001.
23. J.W. Qiu and I. Vitev, hep-ph/0405068.
24. K. Tywoniuk, I. Arsene, L. Bravina, and A.B. Kaidalov, poster, this conference.
25. B. Kopeliovich et al., hep-ph/0501260.
26. I. Vitev, 2005 RHIC&AGS Annual User's Meeting; T. Goldman, M. Johnson, J.W. Qiu, I. Vitev, in preparation.
27. R.C. Hwa, C.B. Yang and R.J. Fries, Phys. Rev. **C71** (2005) 024902.
28. M. Gyulassy, I. Vitev, X.N. Wang and B.W. Zhang, Quark Gluon Plasma 3, editors: R.C. Hwa and X.N. Wang, World Scientific, Singapore (2003) 123-191.
29. Gallmeister *et al.*, Phys. Rev. **C67** (2003) 044905; R.J. Fries, B. Muller, C. Nonaka and S.A. Bass, Phys. Rev. **C68** (2003) 044902; R. Hwa, nucl-th/0501054.
30. J. Dunlop *et al.* (STAR collaboration), these Proceedings.
31. Z. Yin, PhD thesis, Bergen (2004).
32. P. Staszel *et al.* (BRAHMS collaboration), these Proceedings.
33. R. Karabowicz *et al.* (BRAHMS collaboration), these Proceedings.
34. S.S. Adler *et al.* (PHENIX Collaboration), Phys. Rev. Lett. **91** (2003) 072301.
35. I. G. Bearden *et al.* (BRAHMS collaboration), Phys. Rev. Lett. **94** (2005) 162301.
36. J.I. Jørdre, PhD thesis, Bergen (2005).
37. I. G. Bearden *et al.* (BRAHMS collaboration), Phys. Rev. Lett. **93** (2004) 102301.
38. I. Arsene *et al.* (BRAHMS collaboration), poster, this conference.
39. T. Hirano and Y. Nara, Nucl. Phys. **A743** (2004) 305; T. Hirano and Y. Nara, Phys. Rev. **C68** (2003) 064902.
40. A. Dainese, C. Loizides and G. Paic, Eur. Phys. J **C38** (2005) 461.